

P3.4 Investigation of the 31 May 2003 MCS with leading stratiform precipitation from BAMEX

Brandon A. Storm* and Matthew D. Parker
University of Nebraska-Lincoln, Lincoln, Nebraska

1. INTRODUCTION AND BACKGROUND

Mesoscale convective systems (MCSs) account for numerous flash floods, and the degree of flooding that they cause is related to their organizational modes and speeds. Previous work by Parker and Johnson (2000) identified three linear MCSs modes with convective lines and either trailing (TS), parallel (PS), or leading (LS) stratiform precipitation. Parker and Johnson (2000) also found that, on average, LS MCSs had mean lower tropospheric inflow that passed through their pre-line precipitation, referred to as “front-fed” LS (FFLS) systems.

Recent modeling work has given further insight into the structure and dynamics of FFLS systems (Parker and Johnson 2004 a,b,c). FFLS systems have a predominant overturning updraft (Figure 1), whose evolution is influenced by the outflow’s strength and the vertical wind shear. An interesting finding is that inflowing air is actually destabilized as it passes through the pre-line precipitation, leading to a stable and long-lived system (Parker and Johnson 2004b).

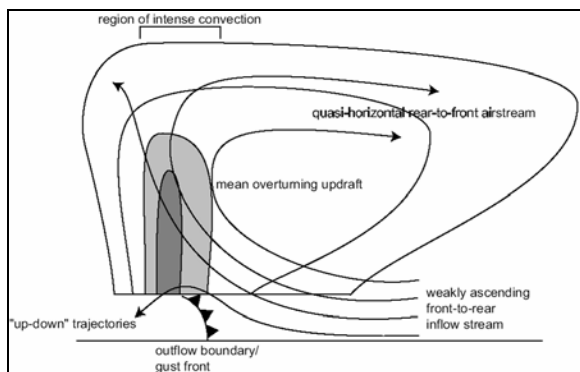


Figure 1: Conceptual model of a front-fed convective line with leading precipitation, viewed in a vertical cross section oriented perpendicular to the convective line and parallel to its motion (Parker and Johnson 2004c).

Very few detailed observational studies of FFLS systems have been undertaken for comparison and verification of the idealized model simulations. However, on 31 May 2003 from 0100 UTC to 0430 UTC an FFLS system was sampled by the Bow Echo and MCV Experiment (BAMEX) over parts of

Illinois and Indiana. The system is divided into two regions, A and B (Figure 2). This is due to differences in the line orientation, system speed, and convective characteristics between the two areas.

Airborne radar and soundings will be used to evaluate the hypothesized roles of system outflow strength and shear on the evolution of the FFLS system, as well as the hypothesized mechanism for destabilization of system inflow by the leading precipitation. This paper will focus on the storm’s evolving structure.

2. DATA

Two airborne radars were utilized on the day under investigation, the NOAA P-3 tail radar and the NRL P-3 ELDORA (Figure 2). For brevity, only the NOAA P-3 radar data are presented here. Dual Doppler analyses were used to retrieve the 3D wind fields, providing high temporal and spatial resolution of the storm’s structure.

GLASS soundings were released from two locations in the system’s path (referred to as G1 and G2; see Figure 2). The soundings were taken approximately hourly, and nearly simultaneously. These data are used to depict the storm-relative flow and vertical wind shear near the system, along with the thermodynamic environment. National Oceanic and Atmospheric Administration (NOAA) Profiler Network (NPN) data were also used. For more information about data available from BAMEX, see Davis et al. (2004).

3. BACKGROUND ENVIRONMENT

A surface low pressure system with an occluded and cold front moved east-southeastward across Wisconsin and Illinois during the late hours of 30 May 2003 (not shown). Supercell storms formed in southern Wisconsin around 2100 UTC 30 May 2003 and developed southward into northern Illinois by 2300 UTC. The system developed into an FFLS system around 0130 UTC 31 May 2003.

The environment had low values of convective available potential energy (CAPE) ahead of the system (Figure 3a). As the system approached the sounding locations, most unstable (MU) CAPE was observed to increase to 924 J kg^{-1} at G1 (Figure 3b). This may be the result of a fundamental

* Corresponding author address: Brandon A. Storm, 210 Bessey Hall, University of Nebraska – Lincoln, Lincoln, NE 68588
Email: bstorm2@bigred.unl.edu

destabilization process that occurs within the LS region, which allows the system to be stable and long-lived. Parker and Johnson (2004b) found that the vertical profile of melting, evaporation, and

consequent ascent in the LS region could remove CIN and add CAPE to the pre-line base state sounding. This aspect of the 31 May 2003 MCS will be investigated more in our ongoing work.

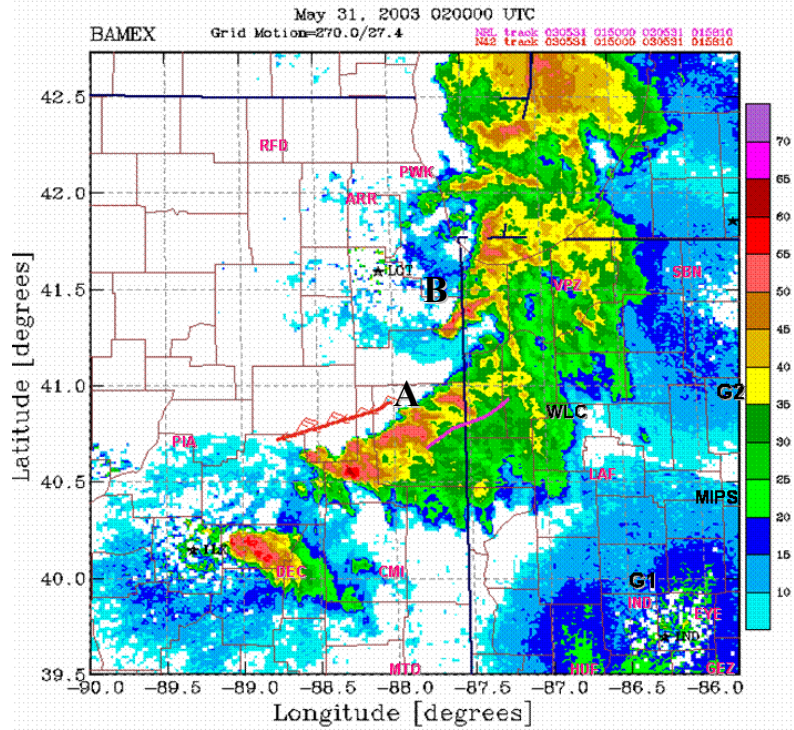


Figure 2. Composite radar reflectivity (dBZ) at the time period 0200 UTC from WSR-88D radars. Flight tracks of NOAA P-3 and NRL P-3 during the time period of 0150 – 0159 UTC are indicated by red and purple line, respectively. Locations of soundings are indicated by G1 and G2 and Wolcott, IN wind profiler site by WLC.

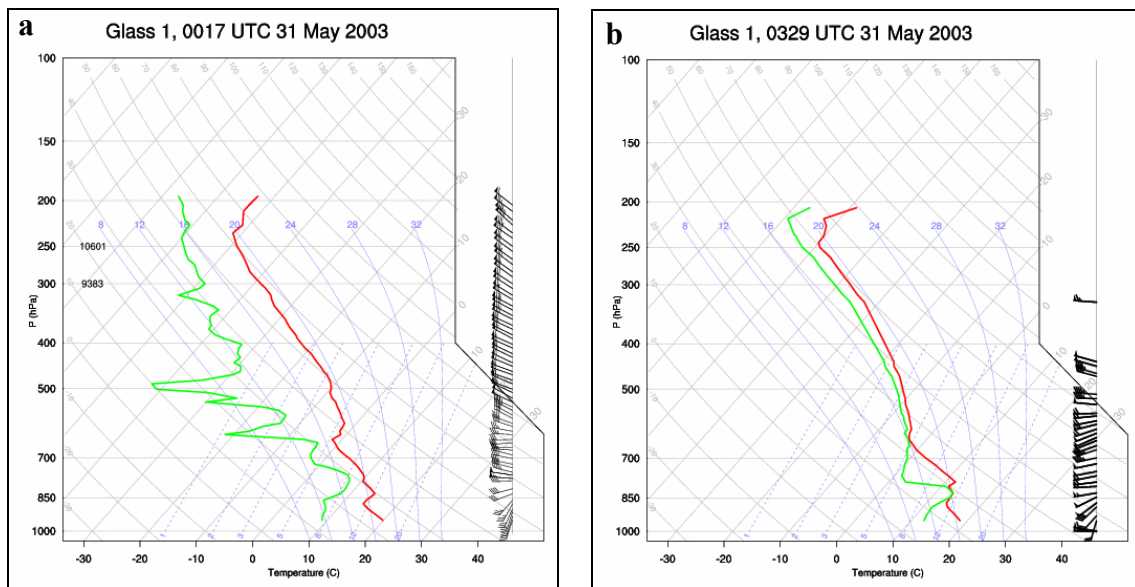


Figure 3. Skew T-ln p plot of rawinsonde observations from G1: (a) 0017 UTC 31 May 2003: mixed-layer (ML)CAPE = 0 J kg⁻¹ and MLCIN = n/a; most unstable (MU) parcel at 772 hPa has MUCAPE = 53 J kg⁻¹ and MUCIN = -8 J kg⁻¹. (b) 0329 UTC 31 May 2003: MLCAPE = 43 J kg⁻¹ and MLCIN = -155 J kg⁻¹; MU parcel at 829 hPa has MUCAPE = 924 J kg⁻¹ and MUCIN = -5 J kg⁻¹; flag=25 m s⁻¹, full barb=5 m s⁻¹, half barb=2.5 m s⁻¹.

4. STORM STRUCTURE AND SHEAR

By 0200 UTC May 31 the system had developed into an FFLS system over eastern Illinois and western Indiana, with the heaviest convection on its southern end (Figure 2). Observations of the FFLS system during its early, mature and dissipating stages are used to depict its basic structure and evolution. Here we present data from 0200, 0300 and 0400 UTC, and also discuss the environmental shear and pre-system flow during the evolving system's lifetime.

4.1 STORM-RELATIVE PRE-SYSTEM FLOW AND SHEAR

Storm-relative pre-system flow and shear values were computed from the NPN station Wolcott, Indiana (WLC), G1, and G2 soundings. We assume that G1 represents region A (Figure 2), the area with more organized convection, while G2 represents region B. WLC is roughly between the two regions.

The system experienced line-perpendicular front-to-rear flow, passing through the leading stratiform region up through 5 km AGL (Figure 5), characteristic of a FFLS system. Little to no along-line flow was observed ahead of the system (not shown). G2 had experienced deeper rearward storm-relative winds than the other sites. In the 5-8 km layer, in which Rutledge and Houze (1987) found bulk transport of MCS hydrometers to be focused, the system experienced mainly rear-to-front storm-relative flow at G1 and WLC. However, G2 experienced mainly front-to-rear flow from 5 – 8 km. This may help explain why region B had a much less archetypal LS structure (Figure 2).

Another significant difference between region A and B is the 0 -3 km vertical wind shear (Table 1). At 0100 UTC, the 0-3 km line-perpendicular shear was significantly larger at G1 and WLC than at G2, which may explain why the convection in region A was stronger and better organized than that in region B (e.g. Rotunno et al. 1988).

4.2 0200 UTC NOAA P-3

The NOAA P-3 radar sampled the southern end of the system around 0200 UTC (Figure 2). Cross-sections were taken perpendicular to the system throughout various updrafts to give a depiction of the storm structure and flow (Figure 5a).

The updrafts' common feature is an overturning updraft, and the cross-sections correspond well to Parker and Johnson's (2004c) conceptual model (Figure 1). Most of the flow is perpendicular to the line (Figures 5 and 6), such that the system is quasi-2D. Interestingly, the convective updrafts were fairly shallow (Figure 6), extending only to 5 – 6 km AGL.

This feature may have resulted from the low environmental CAPE. It appears that most of the updrafts are downshear from the heavy precipitation cores (Figure 5a and 5b). Precipitation develops within the rearward canted part of the updrafts (below 5 km AGL in Figures 6 A,B,C) and is unloaded before the updraft air acquires rear-to-fore momentum and overturns. The leading stratiform precipitation then results from remaining, smaller hydrometers that are advected forward.

The localized higher reflectivities within the stratiform region ahead of the convective line (Figures 6 B and C) are related to upward motions from old updrafts that have been cut off from the low-level inflow and are moving downshear. Such features may take the form of a buoyancy roll (gravity wave). Although not yet well understood, these patches of ascent and enhanced reflectivity also appear in numerical simulations of FFLS systems (e.g. Parker and Johnson 2004a).

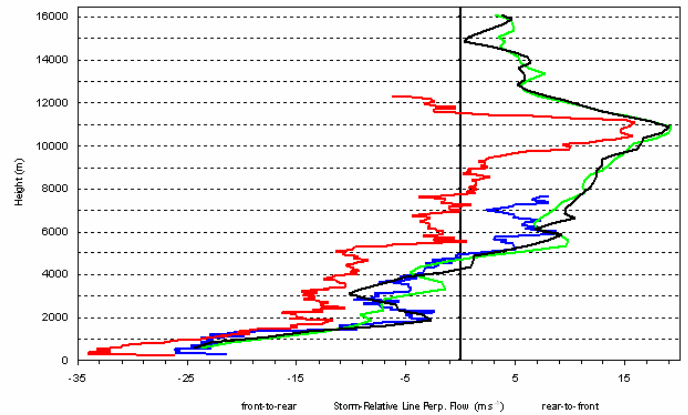


Figure 4. Vertical profiles of storm-relative line-perpendicular winds for; WLC at 0000 UTC (Black), WLC at 0100 UTC (Green), G1 at 0138 UTC (Blue), and G2 at 0125 UTC (Red). Light blue shading indicates 5 – 8 km.

Table 1. Line-perpendicular shear parameters from WLC, G1, and G2 around 0100 UTC, expressed as vector wind differences over specified layers.

Data Source	Parameter	Observed Value (m s^{-1})
G1 (0138 UTC)	0-3 km Line Perp. Shear	18
	0-6 km Line Perp. Shear	29
	3-10 km Line Perp. Shear	21*
WLC (00 UTC)	0-3 km Line Perp. Shear	14
	0-6 km Line Perp. Shear	31
WLC (01 UTC)	3-10km Line Perp. Shear	27
	0-3 km Line Perp. Shear	17
	0-6 km Line Perp. Shear	31
G2 (0125 UTC)	3-10 km Line Perp. Shear	23
	0-3 km Line Perp. Shear	12
	0-6 km Line Perp. Shear	24
	3-10 km Line Perp. Shear	26

*estimated due to missing data

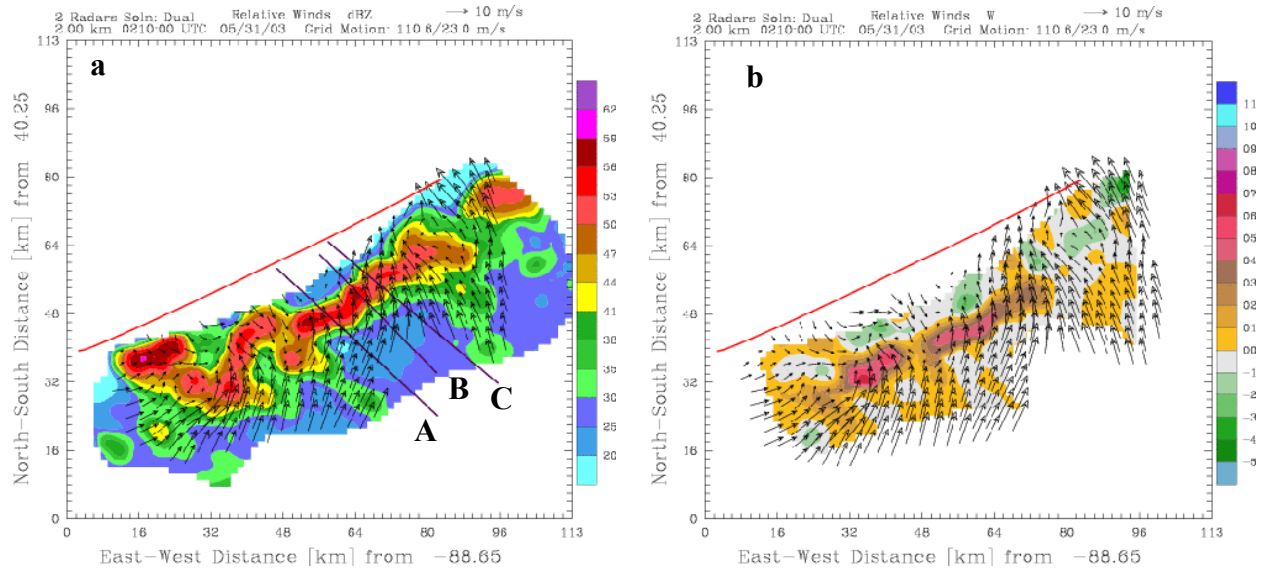


Figure 5. Horizontal analysis of (a) radar reflectivity and system-relative wind flow and (b) vertical air motion at 2.0 km MSL valid at 0210 UTC. Flight track shown in red, same as flight path in Figure 2. Thin black lines are locations of cross sections shown in Figure 6. Reflectivity and vertical air motion contour scale and the 10 m s^{-1} scaling vector for winds are shown to the right and above respectively.

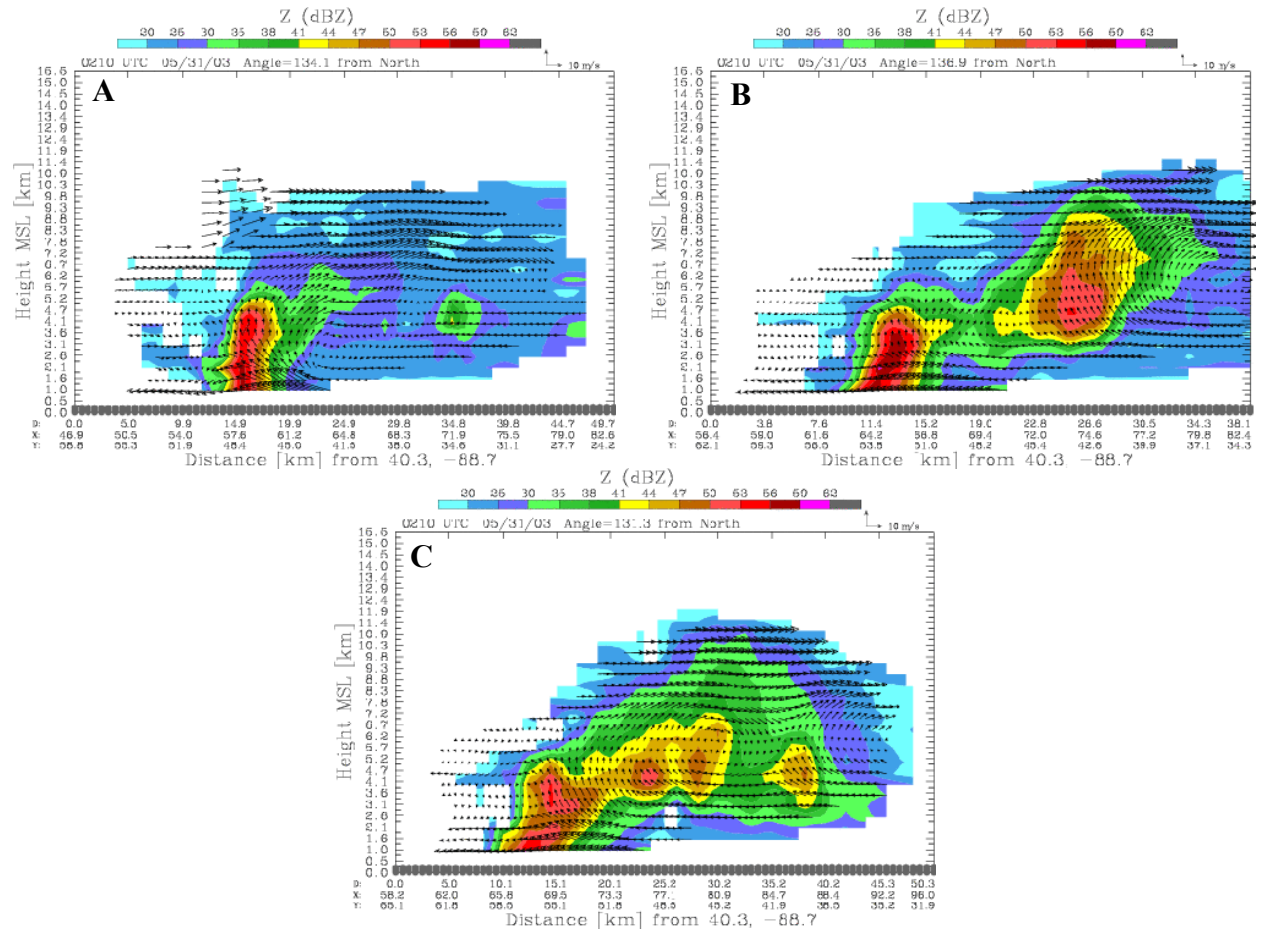


Figure 6. Vertical cross section of reflectivity and system-relative wind through corresponding lines in Figure 5. Reflectivity and vertical air motion contour scale and the 10 m s^{-1} scaling vector for winds are shown above.

4.3 0300 UTC NOAA P-3

The NOAA P-3 sampled roughly the same part of the system at 0300 UTC as it had at 0200 UTC (Figure 7). Low level flow became increasingly parallel to the line, and converged near the high reflectivity returns (Figure 7). The reasoning and significance of increasingly line parallel flow at low-levels will be investigated more in the future.

The updrafts at 0300 UTC tended to lean more strongly upshear than those at 0200 UTC (Figure 8). An overturning updraft was still present. However, a jump updraft and overturning downdraft were also present (Figure 8 and 9), apparently marking the transition from a LS system to a trailing TS system. A trailing stratiform region was developing at 0300 UTC (Figure 8), presumably because the jump updraft now carries some of the hydrometers rearward.

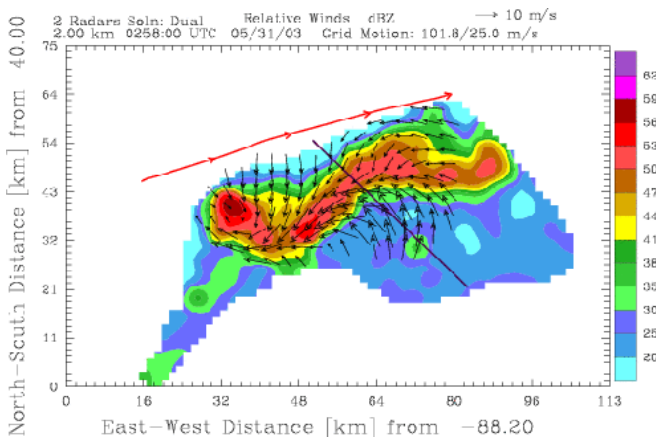


Figure 7. Horizontal analysis of radar reflectivity and system-relative wind flow at 2.0 km MSL valid at 0258 UTC. Flight track shown in red. Thin black line is location of cross sections shown in Figure 8. Reflectivity contour scale and the 10 m s^{-1} scaling vector for winds are shown to the right and above respectively.

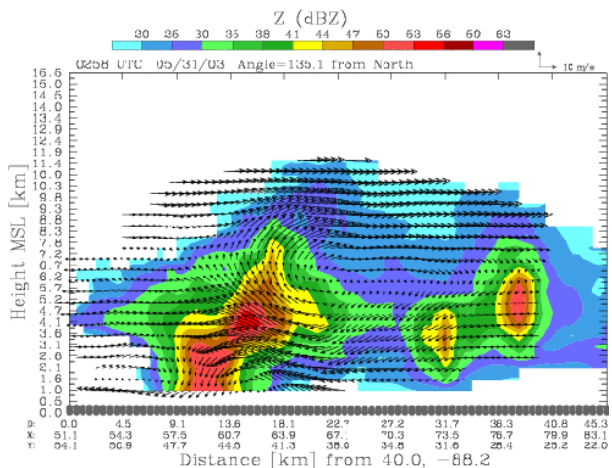


Figure 8. Vertical cross section of reflectivity and system-relative wind through corresponding lines in Figure 7. Reflectivity and vertical air motion contour scale and the 10 m s^{-1} scaling vector for winds are shown to the above.

In contrast to the FFLS systems modeled by Parker and Johnson (2004b), as the 31 May system matured no significant change was noted in the low-level line-perpendicular shear, even as the storm-relative line-perpendicular flow weakened over time. It may be that the cold pool's strength was the key factor in the evolution of this case. The transition from LS to TS structure is a subject of our ongoing investigation.

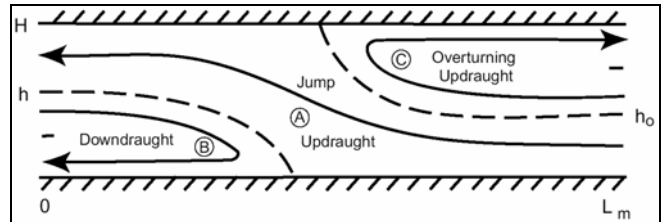


Figure 9. Theoretical two-dimensional model of a convective line depicting both jump and overturning updrafts, redrafted from Moncrieff (1992).

4.4 0400 UTC NOAA P-3

The NOAA P-3 again sampled the southern part of the system around 0400 UTC. The convection was less organized and not as intense as at previous times (Figure 10). The 0400 UTC cross-section shows no evidence of an overturning updraft (Figure 11). The region of TS precipitation continued to develop as a result of an increasingly dominant jump updraft carrying hydrometers rearward. The original, archetypal LS structure was by then almost totally absent. Our continuing investigations will address differences between the near-storm environments at 0200, 0300, and 0400 UTC in order to better explain the dynamical differences between the LS and TS modes, and the transition between them.

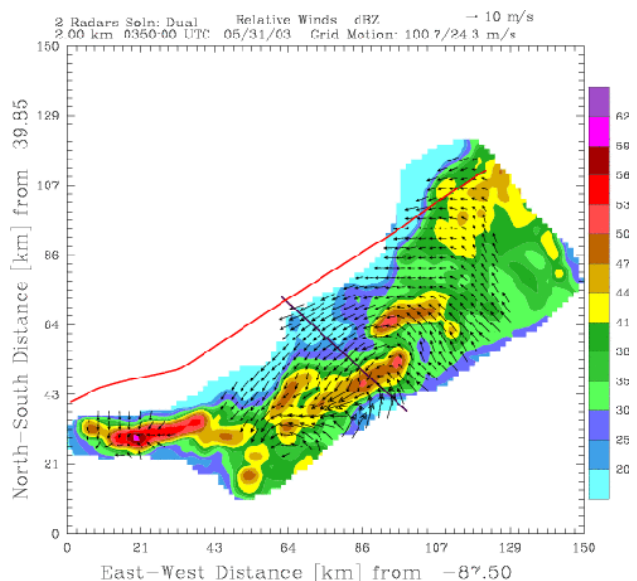


Figure 10. Same as Figure 7, except valid at 0350 UTC.

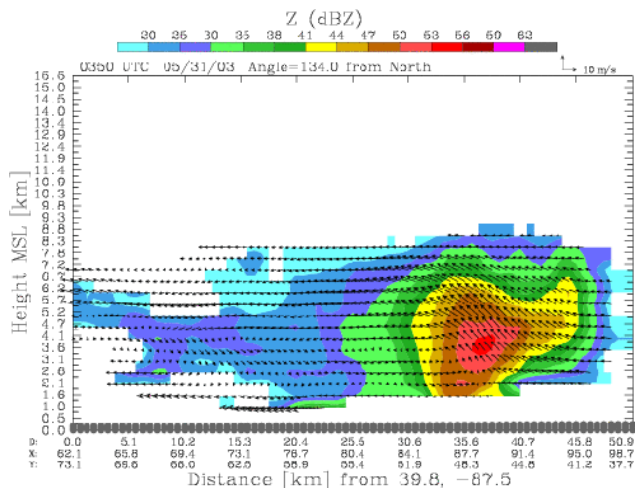


Figure 11. Same as Figure 8, except for location shown in Figure 10.

5.0 CONCLUDING REMARKS

A FFLS system was sampled by the BAMEX on 31 May 2003. The high temporal and spatial resolution of the data provide a detailed look at a front-fed convective line with leading precipitation during its early, transitional, and decaying stages. The conceptual model developed by Parker and Johnson (2004a) in Figure 1 represents the flow structure of the 31 May system in its early stage. As the system matured, alternate flow structures appeared, and the system evolved toward TS structure. It appears that the low-level shear did not change significantly as the system matured, even though weakening line-perpendicular storm-relative flow was evident in the low levels. Our ongoing work will focus on a detailed understanding of the system's controlling dynamics, as well as the possible destabilization mechanism within the leading stratiform region.

ACKNOWLEDGEMENTS

The authors would like to acknowledge Dave Jorgensen for his assistance with the airborne radar data. The research reported here is supported by the National Science Foundation under grant ATM-0349069.

REFERENCES

- Davis, C., and coauthors, 2004: The Bow Echo and MCV Experiment (BAMEX): Observations and opportunities. *Bull. Amer. Meteor. Soc.*, in press.
- Moncrieff, M.W., 1992: Organized convective systems: Archetypal dynamical models, mass and momentum flux theory, and parameterization. *Quart. J. Roy. Meteor. Soc.*, **118**, 819-850.
- Parker, M.D., and R.H. Johnson, 2000: Organizational modes of mid-latitude mesoscale convective systems. *Mon. Wea. Rev.*, **128**, 3413-3436.
- and -----, 2004a: Simulated convective lines with leading precipitation. Part I: Governing dynamics. *J. Atmos. Sci.*, **61**, 1637-1655.
- and -----, 2004b: Simulated convective lines with leading precipitation. Part II: Evolution and maintenance. *J. Atmos. Sci.*, **61**, 1656-1673.
- and -----, 2004c: Structures and dynamics of quasi-2D mesoscale convective systems. *J. Atmos. Sci.*, **61**, 545-567.
- Rotunno, R., J.B. Klemp, and M.L. Weisman, 1988: A theory for strong, long-lived squall lines. *J. Atmos. Sci.*, **45**, 463-485.
- Rutledge, S.A. and R.A. Houze, Jr., 1987: A diagnostic modeling study of the trailing stratiform region of a midlatitude squall line. *J. Atmos. Sci.*, **44**, 2640-2656.